PLoS Pathogens (12/2018)

Carbohydrate, glutathione, and polyamine metabolism are central to *Aspergillus flavus* oxidative stress responses over time

Short Title: *Aspergillus flavus* metabolic responses to oxidative stress

Jake C. Fountain[1,2], Liming Yang[2,3], Manish K. Pandey[4], Prasad Bajaj[4], Danny Alexander[5], Sixue Chen[6], Robert C. Kemerait[2], Rajeev K. Varshney[4], Baozhu Guo[1,*]

[1] USDA-ARS, Crop Protection and Management Research Unit, Tifton, GA 31793, USA;

[2] Department of Plant Pathology, University of Georgia, Tifton, GA 31793, USA;

[3] Nanjing Forestry University, College of Biology and Environmental Science, Nanjing 210037, China;

[4] International Crop Research Institute for the Semi-Arid Tropics (ICRISAT), Hyderabad, Telangana 502324, India

[5] Metabolon, Inc., Durham, NC 27713, USA;

[6] University of Florida, Department of Biology, Genetics Institute, and Plant Molecular & Cellular Biology Program, Gainesville 32611, FL, USA.

Author e-mail addresses: J.C. Fountain: jfount1@uga.edu; L. Yang: yanglim10@163.com; M. Pandey: m.pandey@cgiar.org; P. Bajaj: p.bajaj@cgiar.org; D. Alexander: dalexander@metabolon.com; S. Chen: schen@ufl.edu; R.C. Kemerait: kemerait@uga.edu; R.K. Varshney: r.k.varshney@cgiar.org; B. Guo: baozhu.guo@ars.usda.gov

***Corresponding Author:**
Dr. Baozhu Guo
baozhu.guo@ars.usda.gov

Key Words: *Aspergillus flavus*, aflatoxin, drought stress, oxidative stress, metabolomics

Abstract

The primary and secondary metabolites of fungi are critical for adaptation to environmental stresses, host pathogenicity, competition with other microbes, and reproductive fitness. Drought-derived reactive oxygen species (ROS) have been shown to stimulate aflatoxin production and regulate development in *Aspergillus flavus*, and may function in signaling with host plants. Here, we have performed global, untargeted metabolomics to better understand the role of aflatoxin production in oxidative stress responses, and also explore isolate-specific oxidative stress responses over time. Two field isolates of *A. flavus*, AF13 and NRRL3357, possessing high and moderate aflatoxin production, respectively, were cultured in medium with and without supplementation with 15mM H_2O_2, and mycelia were collected following 4 and 7 days in culture for global metabolomics. Overall, 389 compounds were described in the analysis which were examined for differential accumulation. Significant differences were observed in both isolates in response to oxidative stress and when comparing sampling time points. The moderate aflatoxin-producing isolate, NRRL3357, showed extensive stimulation of antioxidant mechanisms and pathways including polyamines metabolism, glutathione metabolism, TCA cycle, and lipid metabolism while the highly aflatoxigenic isolate, AF13, showed a less vigorous response to stress. Carbohydrate pathway levels also imply that carbohydrate repression and starvation may influence metabolite accumulation at the later timepoint. Higher conidial oxidative stress tolerance and antioxidant capacity in AF13 compared to NRRL3357, inferred from their metabolomic profiles and growth curves over time, may be connected to aflatoxin production capability and aflatoxin-related antioxidant accumulation. The coincidence of several of the detected metabolites in H_2O_2-stressed *A. flavus* and drought-stressed hosts suggests their

potential role in the interaction between these organisms and their use as markers/targets to enhance host resistance through biomarker selection or genetic engineering.

Author Summary

Aspergillus flavus is a fungal pathogen of several important crops including maize and peanut. This pathogen produces carcinogenic mycotoxins known as aflatoxins during infection of plant materials, and is particularly severe under drought stress conditions. This results in significant losses in crop value and poses a threat to food safety and security globally. To combat this, understanding how this fungus responds to environmental stresses related to drought can allow us to identify novel methods of mitigating aflatoxin contamination. Here, we analyzed the accumulation of a broad series of metabolites over time in two isolates of *A. flavus* with differing stress tolerance and aflatoxin production capabilities in response to drought-related oxidative stress. We identified several metabolites and mechanisms in *A. flavus* which allow it to cope with environmental oxidative stress and may influence aflatoxin production and fungal growth. These may serve as potential targets for selection in breeding programs for the development of new cultivars, or for alteration using genetic engineering approaches to mitigate excessive aflatoxin contamination under drought stress.

Introduction

Abiotic stresses such as drought, heat, and osmotic stress have significant effects on the growth of plant pathogenic fungi, and can hinder their capability of infecting host plants. Drought stress in particular has been shown to have significant effects on both fungal pathogenicity and on host resistance to infection with some degree of specificity. For example, the growth of pathogenic

78 fungi such as *Botrytis cinerea* causing gray mold, and *Oidium neolycopersici* causing powdery
79 mildew on tomato are reduced or inhibited under drought stress (Achou et al. 2006; Ramegowda
80 and Senthil-Kumar, 2015). Drought can also influence host metabolic composition and affect
81 interactions with invading pathogens (Lecompte et al. 2017). The growth of microbes in soil
82 environments along with their metabolic profiles and development can also be influenced by
83 drought stress resulting in altered soil ecology and competition among microbes for limiting
84 resources (Schimel et al. 2007). This shows the importance of metabolite accumulation in fungal
85 environmental stress responses and pathogenicity, and the potential for abiotic stresses to
86 regulate host plant immunity.

87 Members of the genus *Aspergillus* have been extensively studied using focused and
88 untargeted metabolomics studies given their role as saprophytes in soil environments, their
89 industrial applications, and their potential as human, animal, and plant pathogens. Examination
90 of the metabolic responses of these fungi have been primarily focused on identifying metabolites
91 involved in fungal growth and development, and the discovery of novel secondary metabolites
92 encoded by silent, conserved gene clusters through both genomic prediction, and induced
93 production using applied stressors or epigenetic modifying compounds (Albright et al. 2015
94 Bertrand et al. 2014; Brakhage, 2013; Scherlach and Hertweck, 2009). This has led to the
95 identification of a number of metabolites with potential pharmaceutical applications, and several
96 involved in the regulation of fungal biology (Amare and Keller, 2014; Calvo et al. 2002; Lopez
97 et al. 2003). However, application of these techniques to study plant pathogenic species of
98 *Aspergillus* have been limited.

99 An example of this is *Aspergillus flavus*, a facultative pathogen affecting crops such as
100 maize and peanut which produces carcinogenic secondary metabolites termed aflatoxins. Annual

losses can exceed $1 billion for US growers, particularly in regions susceptible to drought stress which has been shown to exacerbate aflatoxin contamination (Hill et al. 1983; Mitchell et al. 2016; Scully et al. 2009). Recent examination of developing maize kernels under drought stress also showed that accumulation of polyunsaturated fatty acids, and simple sugars along with decreases in antioxidants such as polyamines occurred in inbred lines sensitive to drought stress and susceptible to aflatoxin contamination (Yang et al. 2018). The same study also showed a greater accumulation of reactive oxygen species (ROS), specifically hydrogen peroxide (H_2O_2), in kernels of the drought sensitive line compared to the drought tolerant line under drought suggesting a correlation between drought tolerance and both ROS accumulation and aflatoxin contamination. Therefore, investigating this correlation between both matrix composition and ROS accumulation with aflatoxin production in *A. flavus* may provide insights into mitigating drought-induced contamination.

Matrix composition has been shown to heavily influence both *A. flavus* growth and aflatoxin production. For example, carbon sources have been found to have a significant effect on aflatoxin production *in vitro* with simple sugars being able to support aflatoxin production by *A. flavus* and *A. parasiticus* while other carbon sources such as peptone can inhibit aflatoxin production in a concentration-dependent manner (Fountain et al. 2015; Yan et al. 2012). Carbon source and availability has also been shown to influence conidiation in *A. flavus* (Fountain et al. 2015). In addition, the accumulation of lipid compounds such as unsaturated fatty acids, and oxylipins in host tissues have been demonstrated to influence aflatoxin production (Burow et al. 1997; Gao et al. 2009; Xue et al. 2003; Zerinque et al. 1996).

During *in vitro* experiments, the same ROS detected by Yang et al. (2018) to accumulate in maize kernels under drought have also been shown to stimulate the production of aflatoxin in

124 both *A. flavus* and *A. parasiticus*, and aflatoxin precursors in *A. nidulans* (Grintzalis et al. 2014;
125 Jayashree and Subramanyam, 2000; Narasaiah et al. 2006; Yin et al. 2013). Variation in
126 oxidative stress tolerance has also been observed among field and mutant isolates of *A. flavus*
127 with isolates exhibiting greater aflatoxin production and more later-stage precursor production
128 tending to tolerate greater levels of oxidative stress compared to less toxigenic or atoxigenic ones
129 (Fountain et al. 2015; Roze et al. 2015). Such variation in stress tolerance and growth patterns
130 may also be characteristic of differences in vegetative compatibility groups (VCGs) which have
131 been shown to vary in host pathogenicity, and competitive ability with other isolates for
132 environmental nutrients (Mehl and Cotty, 2010, 2013). Also, ROS function in reproductive
133 signaling in *Aspergillus spp.* with oxidative responses being closely interconnected with the
134 regulation of reproductive development (Roze et al. 2011). Further, oxidative stress results in
135 extensive metabolic profile alterations to fungi with regards to primary metabolism and
136 antioxidant mechanisms following induction by either ROS or ROS-generating compound
137 application (Sobon et al. 2018; Xu et al. 2018; Zheng et al. 2015).

138 Previous experimentation examining the oxidative stress responses of field isolates of *A.*
139 *flavus* with different levels of aflatoxin production and stress tolerance by our group have shown
140 a high degree of variability among isolates in overall strategies to remediate stress at both the
141 transcript and protein levels (Fountain et al. 2016a, 2016b, 2018). These studies suggested that
142 highly toxigenic isolates may exhibit earlier, more effective oxidative stress remediation
143 mechanisms compared to less toxigenic or atoxigenic isolates. Transcripts and proteins involved
144 in antioxidant protection, carbohydrate metabolism, microbial competitiveness, reproductive
145 development, and the production of other secondary metabolites such as kojic acid and aflatrem
146 were among those differentially expressed in response to oxidative stress. Differences in isolate-

specific oxidative stress responses were also proposed to be due to resource allocation and the regulation of primary and secondary metabolic pathways to mitigate oxidative damage. While these studies provided an extensive overview of transcript and protein-level responses to oxidative stress, they are not fully capable of characterizing changes in final biochemical product levels, and resource allocation over time. Therefore, the objectives of this study were: 1) to identify differentially accumulating metabolites over time to explain isolate-to-isolate variability in oxidative stress responses; 2) to identify metabolic responses that begin to explain the relationship between oxidative stress and exacerbated aflatoxin production; and 3) to identify the metabolites that correspond to host drought responses with potential use in improving host resistance through selection or biotechnology. To accomplish this, we performed a global, untargeted metabolomics analysis of two field isolates of *A. flavus* with different levels of aflatoxin production and their response to oxidative stress over time.

Results

Effects of oxidative stress on isolate growth rates

Two isolates of *A. flavus*, AF13 and NRRL3357, which were previously observed to possess relatively high (up to 35mM H_2O_2) and moderate (up to 20mM H_2O_2) levels of oxidative stress tolerance and aflatoxin production, respectively (Fountain et al. 2015), were selected for this study. The isolate AF13 is a high aflatoxin producing L-strain (sclerotia size >400µm) with a MAT1-2 mating type belonging to the YV-13 vegetative compatibility group (VCG) and relatively high tolerance to oxidative stress (Cotty, 1989; Ehrlich et al. 2007; Fountain et al. 2015). The isolate NRRL3357 is a moderately high aflatoxin producing L-strain with a MAT 1-1 mating type with no currently defined VCG, and moderate tolerance to oxidative stress (Chang et

al. 2012; Fountain et al. 2015). These isolates were examined for conidial oxidative stress tolerance and the effect of oxidative stress on growth rates. Increasing levels of stress caused significant delays in the initial detection (T_i) of isolate growth for both isolates, but to a greater extent in NRRL3357 compared to AF13 at both inoculum levels (Figure 1, Table S1). For AF13, significant growth delays were observed beginning at 10mM H_2O_2 and increasing up to 25mM where growth was completely suppressed at 20,000 conidia/mL (Figure 1A) but not at 80,000 conidia/mL (Figure 1C). However, growth was completely inhibited at 30mM H_2O_2 even at the higher inoculum concentration (Table S1). For NRRL3357, significant delays in growth were also observed at 10mM H_2O_2 while 15mM was completely inhibitory of growth at 20,000 conidia/mL (Figure 1B) but not at 80,000 conidia/mL (Figure 1D). Growth was also completely inhibited at 20mM H_2O_2 at the higher inoculum concentration (Table S1). These inhibitory concentrations of H_2O_2 observed for each isolate were 5 – 10mM less than observed when the isolates were cultured in H_2O_2 amended YES medium in Erlenmeyer flasks with cotton plugs (Fountain et al. 2015).

Differential metabolic alterations in response to oxidative stress over time

Two field isolates of *A. flavus* were selected for global, untargeted metabolomics analysis using an UPLC-MS/MS approach to examine their responses to drought-related, H_2O_2-derived oxidative stress over time. This metabolomics analysis identified 389 distinct metabolites. Functional classification for the detected metabolites was performed based on the Kyoto Encyclopedia of Genes and Genomes (KEGG) database (Kanehisa and Goto, 2000). These metabolites were grouped into nine super pathways with a majority of metabolites being

192 classified as either amino acids (163), lipids (84), nucleotides (54), or carbohydrates (43). These
193 super pathways were further divided into 47 sub-pathways which are described in Table S2.
194 Welch's two-sample t-test was used for differential accumulation analyses to identify
195 metabolites significantly different between oxidative stress treatments, between isolates, or over
196 time (Table 1). Data normalization using DNA or protein content was found to introduce
197 possible skewing in time and isolate effects on metabolite accumulation. Therefore sample mass
198 per unit volume of extraction solvent was used for normalization and these data were used for
199 analysis and interpretation. Both protein and non-protein normalized datasets, and raw data are
200 included in Supplemental File 1. When comparing between stress treatments, AF13 showed 111
201 and 47 metabolites which differentially accumulated at 4 and 7 DAI, respectively. Of these, 27
202 and 64 metabolites were significantly increased and decreased, respectively, in abundance at 4
203 DAI, and 34 and 13 were increased and decreased in abundance, respectively, at 7 DAI. For
204 NRRL3357, 223 and 90 metabolites were differentially accumulated at 4 and 7 DAI,
205 respectively, in response to stress. Of these, 90 and 133 were significantly increased and
206 decreased, respectively, at 4 DAI, and 65 and 25 were increased and decreased in abundance,
207 respectively, at 7 DAI. Time was a highly significant influence on metabolite accumulation with
208 AF13 showing 257 metabolites with significant differences in abundance between 4 and 7 DAI
209 without H_2O_2treatment and 268 with H_2O_2 treatment. In NRRL3357, this was also apparent with
210 243 and 261 metabolites being significantly altered in abundance between 4 and 7 DAI either
211 with or without H_2O_2 treatment, respectively. Comparisons between the isolates are more likely
212 to reflect genetic differences rather than stress response, but more stark differences in numbers of
213 differentially accumulating metabolites could be observed between AF13 and NRRL3357 at 4
214 DAI regardless of H_2O_2 treatment.

These differences in metabolite accumulation were also observed in principal components analyses (Figure 2). The first component was dominated primarily by time effects reflecting significant differences between the 4 and 7 DAI time points. Significant stress effects could also be observed between the isolates with more stark differences observed at 4 DAI. Samples from 7 DAI did not segregate into distinct clusters as seen in samples from 4 DAI. A higher degree of variability between biological replicates was also observed in the 7 DAI samples compared to 4 DAI.

Carbohydrate metabolic responses to oxidative stress

Significant variation in carbohydrate metabolite accumulation was observed in response to oxidative stress in both AF13 and NRRL3357. AF13 showed significant changes in glycolytic compounds glucose and pyruvate with significant decreases ($p < 0.05$) in both compounds at 4 DAI in response to stress with glucose and fructose levels showing marginally significant increases at 7 DAI ($p < 0.10$; Figure 3). NRRL3357 showed significant decreases in both glucose and pyruvate at 4 DAI in response to stress with a significant decrease in pyruvate also detected at 7 DAI. Fructose levels in NRRL3357 were also increased at both time points in response to stress (Figure 3). Time effects showed that pyruvate accumulated in NRRL3357 over time regardless of H_2O_2 treatment, and glucose and fructose were significantly decreased over time with reductions in glucose only seen in non-stressed samples (Supplemental File 1).

Intermediates in the tricarboxylic acid (TCA) cycle were also significantly affected by oxidative stress. NRRL3357 showed significant reductions, particularly at 4 DAI, in citrate, isocitrate, alpha-ketoglutarate, fumarate, and malate in response to oxidative stress (Figure 3). Conversely, AF13 showed no significant changes in TCA intermediate levels in response to

238 oxidative stress with the exception of a significant increase in succinate at 4 DAI. These
239 compounds were, however, seen to generally accumulate over time in the stressed samples when
240 comparing time points (Supplemental File 1).

241 In addition to these pathways, AF13 and NRRL3357 showed significant reductions in
242 trehalose, arabitol, and xylitol in response to oxidative stress at 4 DAI with less significant
243 decreases or no significant differences being observed in response to stress at 7 DAI
244 (Supplemental File 1). Additional metabolic products of arabinose and xylinose, arabinate and
245 xylinate were increased in accumulation in response to stress in both isolates and time points
246 (Supplemental File 1). Increases in amino sugars were also observed in both isolates, particularly
247 at 4 DAI in response to stress (Supplemental File 1).

248

249 **Amino acid metabolic responses to oxidative stress**

250 Significant changes in the accumulation of amino acids and their derivatives were observed in
251 both isolates in response to oxidative stress over time. Changes in primary amino acids were
252 proportional to changes in their precursors with more significant changes occurring in
253 NRRL3357 compared to AF13 (Figure 3; Supplemental File 1). In particular, changes in
254 aromatic amino acid precursors in the tryptophan and histidine pathways were observed in
255 NRRL3357 in response to oxidative stress although the levels of tryptophan and histidine were
256 unchanged or reduced, respectively, in the same conditions (Supplemental File 1). In addition,
257 the tryptophan derivative kynurenine was increased in NRRL3357 at both time points in
258 response to oxidative stress, but not in AF13 (Supplemental File 1). Proline levels were also
259 increased in NRRL3357 at 7 DAI in response to stress (Supplemental File 1). Among the amino

acid derivatives, those involved in glutathione, polyamine, and sulfur metabolism were among the most differentially accumulating in response to oxidative stress.

Glutathione metabolism was significantly regulated in both isolates but to a greater extent in NRRL3357 compared to AF13 (Figure 3). Significant increases in 5-oxoproline, ophtalmate, oxidized glutathione (GSSH), and cysteine-glutathione disulfide were observed in NRRL3357 in response to increasing stress (Figure 3). AF13 showed marginally significant ($p < 0.10$) increases in accumulation of only 5-oxoproline and ophtalmate were see at 7 DAI in response to stress. Direct comparison of levels between these isolates showed that AF13 accumulated significantly greater levels of GSSH and cysteine-glutathione disulfide at 4 DAI compared to NRRL3357 in the absence of oxidative stress, and equivalent and greater levels, respectively, of each when under oxidative stress (Supplemental File 1). When comparing time point measurements, 5-oxoproline, ophtalmate, and GSSG showed significant reductions in accumulation in both isolates and treatments (Supplemental File 1). Significant changes were also found among the gamma-glutamyl amino acids which were significantly reduced in AF13 at 4 DAI in response to stress, but tended to be either unchanged or increased in accumulation in NRRL3357 in response to stress (Figure 3).

In addition to glutathione, other sulfur-containing amino acids and their metabolites were significantly regulated in response to oxidative stress (Figure 4). Significant reductions in methionine levels were observed in both isolates at 4 DAI in response to oxidative stress. S-adenosylmethionine (SAM), an important signaling compound, was also significantly regulated in response to oxidative stress showing increasing accumulation at 7 DAI in both isolates, and a significant decrease at 4 DAI in NRRL3357 (Figure 4). 5-methylthioadenesine (MTA) also exhibited a similar pattern of accumulation to SAM. In addition to methionine derivatives,

283 cysteine also serves as a precursor to the antioxidant compound taurine which was significantly
284 increased in both isolates at 4 DAI and in AF13 at 7 DAI in response to oxidative stress. A
285 taurine precursor, 3-sulfo-L-alanine, was also significantly increased in both isolates and time
286 points in response to oxidative stress (Figure 4).

287 Polyamine metabolites were also significantly regulated in response to oxidative stress in
288 both isolates. Ornithine showed significant reduction in AF13 at 4DAI while putresine showed
289 the same in NRRL3357 in response to oxidative stress while the immediate precursor to
290 ornithine, N-alpha-acetylornithine, was increased in both isolates at 4 DAI (Figure 4;
291 Supplemental File 1). These compounds are precursors to both spermidine and N-acetylputresine
292 which showed significant increases in both isolates in response to oxidative stress. N-
293 acetylputresine is a part of butanoate metabolism and used for the biosynthesis of gamma-
294 aminobutanoate (GABA) which showed marginally significant changes in abundance in response
295 to oxidative stress (Figure 4).

296

297 **Fatty acid metabolic responses to oxidative stress**

298 Several fatty acids and their derivatives were also significantly regulated in response to H_2O_2-
299 stress over time. Significant regulation of saturated and mono- and poly-unsaturated fatty acid
300 accumulation were primarily observed in NRRL3357 in response to stress (Figure 5). Significant
301 increases in the saturated fatty acids pentadecanoic acid (15:0) and heptadecanoic acid (17:0)
302 were seen at 7 and 4 DAI, respectively, in NRRL3357 in response to stress (Figure 5). Similarly,
303 significant increases in several unsaturated fatty acids were also seen in NRRL3357 (Figure 5).
304 While no significant regulation of these fatty acids was seen in AF13 in response to oxidative

stress within each time point, significant depletion of these fatty acids was observed in both isolates over time with or without the presence of oxidative stress (Supplemental File 1).

Other fatty acid derivatives were also found to differentially accumulate in the isolates under oxidative stress. In AF13, betaine, an ethanolamine derivative, was significantly decreased under oxidative stress at 4 DAI (Figure 5). Several phospholipids such as glycerophosphoglycerol were also found to be differentially accumulating in response to oxidative stress in both isolates (Supplemental File 1). Ergosterol levels were found to be significantly decreased under stress in AF13 at 7 DAI and in NRRL3357 at 4 DAI. There was no significant change in ergosterol levels over time in either treatment, but AF13 accumulated significantly more than NRRL3357 at 4 DAI in both treatments, while at 7 DAI AF13 was found to have more only in the non-stressed control (Supplemental File 1).

Other compounds regulated in response to oxidative stress

In addition to amino acids, carbohydrates, and lipids, other classes of compounds were found to differentially accumulate in response to increasing oxidative stress over time in both isolates. Among cofactors and electron carriers, carnitine and related metabolites were significantly reduced in both isolates at 4 DAI in response to stress, but showed significant increases over time under stress and was present in higher concentrations in AF13 compared to NRRL3357 (Supplemental File 1). Several B vitamins with potential antioxidant activity were also regulated in response to stress including thiamin (B1), riboflavin (B2), and pyridoxine (B6) (Supplemental File 1). Several nucleotide derivatives were also differentially accumulated in response to stress such as adenosine 5'-monophosphate (AMP) which was significantly increased in AF13 at 4 DAI in response to stress, but was significantly depleted in both isolates and treatments over time

328 (Supplemental File 1). Terpenoid and isoterpenoid precursors were also found to differentially
329 accumulate under stress with mevalonate along with its immediate precursor, 3-hydroxy-3-
330 methylglutarate, and its lactone form, mevalonolactone, showing significant increases in
331 response to stress in AF13 at 7 DAI and in NRRL3357 at 4 and 7 DAI (Supplemental File 1).
332
333 **Discussion**
334 Drought stress is one of the primary factors contributing to the exacerbation of pre-harvest
335 aflatoxin contamination in the field. Drought stress has been shown to significantly alter the
336 metabolic composition of maize kernels during earlier stages of development resulting in
337 increased levels of free simple sugars, oxylipins, free fatty acids, and signaling compounds
338 including ROS including H_2O_2, superoxide (O_2^-), and hydroxyl ions (OH^-) (Yang et al. 2015,
339 2018). These ROS have also been found to stimulate and be required for aflatoxin production
340 (Jayashree and Subramanyam, 2000). These observations served as the impetus to investigate
341 responses of *A. flavus* isolates with varying levels of aflatoxin production to drought-related
342 oxidative stress and the metabolite level over time.
343 Aflatoxin production capability has been previously correlated with *A. flavus* isolate
344 oxidative stress tolerance (Fountain et al. 2015; Roze et al. 2015). When examining the growth
345 rates and behavior of *A. flavus* isolates under oxidative stress AF13, a highly toxigenic isolate,
346 was found to exhibit higher levels of oxidative stress tolerance and growth under stress compared
347 to NRRL3357, a moderately high toxigenic isolate (Figure 1). Aflatoxin production and the
348 reactions in the biosynthetic pathway are suspected to result in increased conidial oxidative stress
349 tolerance due to stimulating additional antioxidant enzyme production, or through the
350 consumption of ROS during production (Fountain et al. 2016a; Roze et al. 2015). Given this,

conidial antioxidant enzyme activity may have contributed here. To further examine this, growth curve analyses was performed with different inoculum concentrations, and showed that growth for both isolates occurred at elevated H_2O_2 levels when the inoculum was increased from 20,000 conidia/mL as described by Meletiadis et al. (2001) to 80,000 conidia/mL used here as inoculum for cultures used for metabolomics analysis. Interestingly, even with the increased conidia concentration, observed stress tolerance remained approximately 5 mM less than the maximum observed in the previous study. While this may be an artifact of performing the assay in a sealed microplate with potentially limited oxygen availability, the overall trend was consistent with previous observations of each isolate's tolerance to oxidative stress (Clevstrom et al. 1983; Fountain et al. 2015; Jayashree and Subramanyam, 2000).

When examining overall metabolite accumulation patterns, NRRL3357 displayed approximately double the number of differentially accumulating metabolites compared to AF13 in response to oxidative stress with both isolates exhibiting greater numbers at 4DAI compared to 7 DAI (Table 1). This pattern mirrors observed numbers and functional classifications of differentially expressed transcripts and proteins for these isolates in response to similar levels of oxidative stress in our previous transcriptome and proteome studies (Fountain et al. 2016a, 2016b, 2018). Here, significant differences in metabolite accumulation were detected within and between time points in both isolates, and sampling time was one of the major grouping factors in the PCA analysis (Table 1; Figures 2 and S1). These time course influences may be due to differences in isolate growth patterns and, presumably, timing and vigor of oxidative stress remediation mechanisms. As indicated by the growth curve analysis (Figure 1; Table S1), earlier initiation of growth in AF13 compared to NRRL3357 may be the result of earlier, more vigorous lag phase or conidial oxidative stress remediation processes. Therefore, sampling at 4 DAI for

374 both isolates would describe actively growing and responding tissues while sampling at 7 DAI
375 would describe stationary state responses in AF13 having already remediated the majority of
376 oxidative stress while NRRL3357 would still be actively growing and responding to stress.
377 Examining the isolate-specific responses to oxidative stress, there were significant
378 differences in carbohydrate accumulation. Both glycolysis and TCA cycle intermediates were
379 significantly altered in accumulation in response to oxidative stress in these isolates, but to
380 differing degrees. NRRL3357 displayed increased demand for TCA intermediates showing
381 significant decreases in most quantified metabolites in the cycle while AF13 showed no
382 significant differences (Figure 3). These compounds have been shown to provide some
383 antioxidant benefit when supplemented to cultured neuronal cells (Sawa et al. 2017), though a
384 more likely explanation is the use of these compounds in the synthesis of amino acids and/or
385 their derivatives involved in oxidative stress remediation. Increases in glucose and fructose under
386 stress in both isolates may also be reflective of higher levels of metabolic demand for simple
387 sugars, and the beginnings of carbon starvation leading to gluconeogenesis (Dijkema et al. 1985;
388 Lima et al. 2014), particularly at 7 DAI (Figure 3).
389 When examining time course effects, the accumulation of these compounds in stressed
390 samples may also be indicative on increased energy demand and the need to maintain redox
391 homeostasis through the generation of reduced coenzymes for oxidative phosphorylation such as
392 NADH and NADPH (Kapoor et al. 2015). Significant reductions in their accumulation in
393 NRRL3357 under stress (Figure 3) could, therefore, partially explain the reduced growth rate,
394 and observed ongoing stress responses compared to AF13. Also of interest, the pentose
395 phosphate pathway has been shown to be involved in oxidative stress responses in yeast, and
396 amino sugars such as ribonate are also involved in the generation of reduced coenzymes used for

redox homeostasis (Campbell et al. 2016; Juhnke et al. 1996). These reduced coenzymes, particularly NADPH, are also critical for the activity of polyketide synthases which may also impact aflatoxin production levels under oxidative stress (Huang et al. 2009; Kletzien et al. 1994; Shih and Marth, 1974).

Changes in amino acid metabolite levels appeared to form the basis of a majority of the oxidative stress remediation processes employed by these isolates constituting the bulk of directly antioxidant compounds and mechanisms. Amino acids such as proline have been previously shown to be involved in osmotic, drought, and oxidative stress tolerance in fungi and plants and were increased in abundance in NRRL3357 (Chen and Dickman, 2005; Szabados and Savoure, 2009). Also in NRRL3357, the tryptophan derivative kynurenine was increased and may also contribute to stress remediation. Disruption of kynurenine 3-monooxygenase, a central enzyme in kynurenine metabolism, in *Botrytis cinerea* has been shown to increase tolerance to H_2O_2-derived oxidative stress and host pathogenicity while negatively affecting growth and development (Zhang et al. 2018).

Glutathione pathway components were among the most significantly altered in response to oxidative stress in both isolates, though to a greater extent in NRRL3357 which can be seen in the higher accumulation of oxidized glutathione, 5-oxoproline, and ophthalmate in NRRL3357 under stress which were not seen in AF13 (Figure 3). This pathway in conjunction with enzymes such as catalases and thioredoxin reductases and peroxidases serve as the primary means of redox homeostasis and oxidative stress alleviation for eukaryotes (Breitenbach et al. 2015). Glutathione metabolism has been previously linked to both development and aflatoxin production in *Aspergillus spp*. Huang et al. (2009) showed that treatment of *A. flavus* with an ethylene-producing compound resulted in increases in GSH/GSSH ratios, oxidative stress

420 remediation, and significant reductions in aflatoxin biosynthetic gene expression and aflatoxin
421 production. Reduced glutathione accumulation has also been associated with asexual and sexual
422 development in *A. nidulans* thioredoxin A (*AnTrxA*) mutants with applied GSH resulting in
423 restored conidiation and early induction of cleistothecia formation following long-term, low
424 concentration application (Thon et al. 2007). Given this relationship between glutathione,
425 development, and mycotoxin production, this mechanism may be lending to distinctive growth
426 patterns and aflatoxin production levels in these isolates which represent diverse VCGs and
427 mating types and warrants further investigation (Horn, 2007; Mehl and Cotty, 2010, 2013).
428 Sulfur-containing amino acids such as cysteine and methionine, and their derivatives
429 were also differentially accumulated in response to oxidative stress (Figure 4). These compounds
430 have antioxidant benefits, and also function in important signaling capacities. Taurine, an
431 antioxidant compound (Jong et al. 2012), was shown to accumulate in both isolates under stress
432 along with its immediate precursor 3-sulfo-L-alanine which may supplement other antioxidant
433 pathways (Figure 4). The detected signaling compounds, SAM and MTA, are closely tied to
434 polyamine biosynthesis which was also significantly regulated by oxidative stress. Polyamines
435 such as putresine and spermidine differentially accumulated in this experiment (Figure 4), and
436 have been found to function in oxidative stress responses either by scavenging ROS, inhibiting
437 ROS-generating enzymes, or functioning in signal transduction to promote antioxidant
438 mechanisms (Valdes-Santiago and Ruiz-Herrera, 2014). S-adenosylmethionine is required for
439 the production of polyamines and MTA is produced from decarboxylated SAM by spermidine
440 synthase and spermine synthase with accumulating MTA being able to inhibit these enzymes to
441 prevent the generation of H_2O_2-derived oxidative stress due to polyamine back-conversion
442 (Avila et al. 2004). Therefore, polyamine metabolism along with glutathione metabolism form a

443 coordinated basis for regulating cellular redox potential in *A. flavus* in response to oxidative
444 stress and may assist in coordination of both reproductive development and mycotoxin
445 production.

446 Fatty acids were also significantly altered in accumulation in response to oxidative stress.
447 This is particularly true for mono- and poly-unsaturated fatty acids which tended to be increased
448 in abundance in NRRL3357 in response to stress, but not in AF13 (Figure 5). Unsaturated fatty
449 acids have been found to be suitable substrates for aflatoxin production by *A. flavus* and *A.*
450 *parasiticus*, and their byproducts have been shown to regulate aflatoxin production and
451 development (Fanelli and Fabbri, 1989; Tsitsigiannis and Keller, 2007). For example, linoleic
452 acid derivatives known as Psi factors have been shown to regulate both asexual and sexual
453 sporulation in *A. flavus* and *A. nidulans* (Calvo et al. 1999), and oxylipins function in signaling
454 for development, mycotoxin production, and host interactions (Affeldt et al. 2012; Fischer and
455 Keller, 2016; Gao et al. 2009). In addition to signaling, free fatty acids also serve as important
456 sources of energy, and can be catabolized to produce other macromolecules. Here, a majority of
457 unsaturated lipids were depleted over time in control and stressed conditions in both isolates
458 likely to provide energy and components for repairing and responding to oxidative stress
459 (Supplemental File 1). These fatty acids are also important for maintaining membrane integrity
460 and fluidity under environmental stress conditions. For example, dienoic fatty acids have been
461 shown to function in preserving membrane fluidity in yeast under freezing and salt stresses
462 (Rodriguez-Vargas et al. 2007).

463 Along with these major classes of metabolites, several cofactors and secondary
464 metabolites were also differentially accumulated in response to stress (Supplemental File 1). Of
465 particular interest were mevalonate and related terpenoid compounds which were increased in

466 both isolates in response to oxidative stress. These compounds are precursors to some isoprenoid
467 mycotoxins such as aflatrem whose biosynthetic genes have been found to be upregulated in
468 response to oxidative stress in these isolates (Fountain et al. 2016a, 2016b). In addition,
469 mevalonate and its derivatives have been shown to link the biosynthetic pathways for ergosterol
470 and ornithine-derived siderophores, and interruption of this link results in reduced tolerance to
471 oxidative stress, siderophore production, and virulence in *A. fumigatus* (Yasmin et al. 2011).
472 These compounds differentially accumulating in these isolates of *A. flavus* mirror
473 those observed in other *Aspergillus spp.* such as *A. oryzae* (Singh et al. 2018) and provide
474 potential insights into putative approaches to enhance host resistance under drought stress. We
475 hypothesized that excessive ROS generated in drought sensitive host plants during drought stress
476 may contribute to enhancing susceptibility to aflatoxin contamination (Fountain et al. 2014;
477 2015). In addition, the metabolic pathways employed by *A. flavus* in remediating oxidative stress
478 seen in this study parallel those employed by host plants such as maize in countering drought
479 stress in developing kernel tissues (Yang et al. 2018). Given this relationship, the manipulation
480 of host tissue composition may be a viable approach to improve aflatoxin contamination
481 resistance through two possible methodologies. The first method is biomarker selection
482 employed in breeding programs (Fernandez et al. 2016). For aflatoxin mitigation, enhanced
483 accumulation of antioxidant compounds in host plant tissues corresponding to those observed in
484 *A. flavus* such as glutathione pathway components, polyamines, or simple sugar content could be
485 selected for in conventional and molecular breeding programs. The second method is genetic
486 engineering including both genome editing and transgenic approaches to manipulate the
487 expression of host plant enzymes to modify kernel composition to reduce stress on infecting A.
488 flavus under drought. These technologies could also be used to enhance host plant antioxidant

489 potential through increased antioxidant enzyme expression, antioxidant compound production, or
490 aflatoxin inhibitor production. This would also have the added potential benefit of reduced
491 drought-related kernel abortion and filling reduction due to oxidative damage.
492
493 **Materials and Methods**
494 **Isolate collection**
495 The isolates used in this study were obtained as follows. AF13 was requested from Dr. Kenneth
496 Damann, Department of Plant Pathology and Crop Physiology, Louisiana State University,
497 Baton Rouge, LA. NRRL3357 was requested from the USDA National Culture Repository,
498 Peoria, IL. All isolates were shipped on PDA and transferred to V8 agar as previously described
499 (Fountain et al. 2018). Agar plugs containing fresh conidia were taken along the growing edge of
500 the colonies and stored in sterile water and 20% (v/v) glycerol at 4 and -20°C, respectively, until
501 used.
502
503 **Culture conditions and tissue collection**
504 Isolate conidia suspensions were used to inoculate V8 agar plates, and were incubated at 37°C
505 for 5 days. Conidia were then harvested using sterile 0.1% (v/v) Tween 20 and a sterile loop to
506 make a fresh conidia suspension (~2.0 x 10^7 conidia/mL) for use as inoculum. For each isolate,
507 100 µL of conidial suspension was then used to inoculate stationary liquid cultures of 50 mL
508 yeast extract-sucrose medium (YES; 2% yeast extract, 1% sucrose) in 125mL Erlenmeyer flasks
509 amended with H_2O_2 (3% stabilized solution) to a final concentration of either 0 or 15mM and a
510 final conidia concentration of ~8.0 x 10^4 conidia/mL. The flasks were plugged with sterile cotton
511 and incubated at 30°C in the dark. Mycelial mats were then harvested for each isolate and H_2O_2

512 treatment at 4 and 7 days after inoculation (DAI). Five repeat cultures representing five
513 biological replicates were harvested for each isolate, treatment, and time point. A detailed
514 description of the experiment design can be found in Figure S1. Harvested mycelia mats were
515 immediately flash frozen in liquid nitrogen and ground into a fine powder using sterile, chilled
516 mortar and pestles. The ground tissue (~1g) was then transferred to a sterile 2.0mL
517 microcentrifuge tube and stored at -80°C until use in metabolomics analysis.
518
519 **Metabolomic profiling**
520 Collected and ground mycelia tissues were used for global, unbiased metabolomics by
521 Metabolon (Morrisville, NC, USA) as described by Yang et al. (2018) and Lin et al. (2017).
522 Briefly, 50 mg of tissue from each sample were prepared using an automated MicroLab STAR
523 system (Hamilton, Reno, NV, USA) during which QC standards were added for downstream
524 normalization. Metabolites and proteins were extracted in methanol in a GenoGrinder 2000
525 (Glen Mills, Clifton, NJ, USA) followed by centrifugation for metabolite isolation and protein
526 separation. Each extract was then divided into 5 fractions and used for reverse phase (RP)/ultra-
527 performance liquid chromatography (UPLC)-tandem mass spectrometry (MS/MS) with positive
528 ion mode electrospray ionization (ESI), RP/UPLC-MS/MS with negative ion mode ESI, and
529 HILIC/UPLC-MS/MS with negative ion mode ESI. One fraction from each extract was reserved
530 as a backup. All methods employed either an ACQUITY UPLC (Waters, Milford, MA, USA) or
531 a Q-Exactive High Resolution/Accuracy Mass Spectrometer with a heated electrospray
532 ionization (HESI-II) source and an Orbitrap Mass Analyzer (ThermoFisher, Waltham, MA,
533 USA). A detailed description of methods and procedure for data acquisition, metabolite
534 acquisition, quantitation, and data analysis can be found in Supplemental File 2.

535

536 **Growth curve assay**

537 A growth curve assay was performed for the isolates used for metabolomics analysis under
538 H_2O_2-derived stress using a microtiter plate method as described by Meletiadis et al. (2001).
539 Both isolates were cultured on V8 agar for 7 days at 30°C in the dark. Agar plugs were collected
540 along the growing edge of the colonies and placed into amber bottles containing ~5.0 mL 0.1%
541 (v/v) Tween 20 and gently shaken to suspend conidia. The concentration of each conidial
542 suspension was measured using a hemocytometer, and used to prepare inoculum for each isolate
543 with at two concentrations of 2.0 x 10^4 conidia/mL as described by Meletiadis et al. (2001) and
544 8.0 x 10^4 conidia/mL as used for the present metabolomics assay. A 96-well flat bottom
545 microtiter plate was then prepared by filling each well with 100 µL of double strength YES
546 medium (4% yeast extract, 2% sucrose) amended with 0, 20, 30, 40, 50, or 60 mM H_2O_2. For
547 each inoculum, 100 µL was added to each the prepared wells resulting in a standard YES
548 concentration and a final concentration of 0, 10, 15, 20, 25, or 30 mM H_2O_2. Three replicate
549 wells were inoculated for each isolate and treatment combination. For non-inoculated wells, 100
550 µL of 0.1% Tween 20 was added in place of inoculum. The plate was sealed with optically-clear
551 tape and incubated at 30°C in the dark without shaking in a Synergy HT plate reader (Biotek,
552 Winooski, VT, USA). Optical density at 405 nm (OD_{405}) was recorded every 15 min for 100 hr.
553 The average of the OD_{405} for the non-inoculated wells was then subtracted from each
554 measurement to remove background absorbance.

555

556 **Data analysis**

Raw data obtained from UPLC-MS/MS analyses were peak-identified and QC corrected based on the Metabolon Laboratory Information Management System (LIMS) which contains identifying information for >4500 standard compounds. Quantitation and differential accumulation analyses were performed as described by Lawton et al. (2008), Lin et al. (2017), and Rao et al. (2014) using ArrayStudio and R (v3.4.0). Heatmaps and principal components analyses were performed using MultiExperiment Viewer (MeV, v4.9.0). Functional enrichment analyses were performed with Blast2GO (Conesa et al. 2005), and metabolic pathways were identified based on the KEGG database (Kanehisa and Goto, 2000). Pearson correlation analyses of the detected metabolites was performed using R (v3.4.0) and RStudio (v1.1.423). For the growth curve analysis, Gen3 software (Biotek) was then used to calculate the highest OD (OD_{max}), and average time of initial detection at a defined threshold of $OD_{405} = 0.2$ (T_i).

Acknowledgements

We would like to thank Billy Wilson and Hui Wang for technical assistance in the laboratory. This work is partially supported by the U.S. Department of Agriculture Agricultural Research Service (USDA-ARS), USDA National Institute for Food and Agriculture (USDA-NIFA), the Georgia Agricultural Commodity Commission for Corn, the National Corn Growers Association Aflatoxin Mitigation Center of Excellence (AMCOE), the Georgia Peanut Commission, and The Peanut Foundation. Mention of trade names or commercial products in this publication is solely for the purpose of providing specific information and does not imply recommendation or endorsement by the USDA. The USDA is an equal opportunity employer and provider.

Author Contributions

JCF performed the culture experiments and data analyses, and wrote the manuscript. LY, MKP, and PB assisted in data analysis and in project discussions. DA performed the metabolomics experiment and assisted in data analysis. SC, RCK, and RKV contributed to project discussions and assisted with revision of the manuscript. BG conceived the project, planned, secured extramural funds, and revised and submitted manuscript.

Conflict of Interest

The authors declare no conflict of interests.

References

1. Achuo EA, Prinsen E, Höfte M. Influence of drought, salt stress and abscisic acid on the resistance of tomato to *Botrytis cinerea* and *Oidium neolycopersici*. Plant Pathol. 2006;55: 178-186.
2. Ramegowda V, Senthil-Kumar M. The interactive effects of simultaneous biotic and abiotic stresses on plants: mechanistic understanding from drought and pathogen combination. J. Plant Physiol. 2015;176: 47-54.
3. Lecompte F, Nicot PC, Ripoll J, Abro MA, Raimbault AK, Lopez-Lauri F, Bertin N. Reduced susceptibility of tomato stem to the necrotrophic fungus *Botrytis cinerea* is associated with a specific adjustment of fructose content in the host sugar pool. Ann. Bot. 2017;119: 931-943.
4. Schimel J, Balser TC, Wallenstein M. Microbial stress-response physiology and its implications for ecosystem function. Ecology. 2007;88: 1386-1394.
5. Albright JC, Henke MT, Soukup AA, McClure RA, Thomson RJ, Keller NP, Kelleher NL. Large-scale metabolomics reveals a complex response of *Aspergillus nidulans* to epigenetic perturbation. ACS Chem. Biol. 2015; 10: 1535-1541.
6. Bertrand S, Bohni N, Schnee S, Schumpp O, Gindro K, Wolfender JL. Metabolite induction via microorganism co-culture: a potential way to enhance chemical diversity for drug discovery. Biotechnol. Adv. 2014;32: 1180-1204.
7. Brakhage, AA. Regulation of fungal secondary metabolism. Nat. Rev. Microbiol. 2013;11: 21-32.
8. Scherlach K, Hertweck C. Triggering cryptic natural product biosynthesis in microorganisms. Org. Biomol. Chem. 2009;7: 1753-1760.
9. Amare MG, Keller NP. Molecular mechanisms of *Aspergillus flavus* secondary metabolism and development. Fungal Genet. Biol. 2014;66: 11-18.
10. Calvo AM, Wilson RA, Bok JW, Keller NP. Relationship between secondary metabolism and fungal development. Microbiol. Mol. Biol. Rev. 2002;66: 447-459.

11. López JC, Pérez JS, Sevilla JF, Fernández FA, Grima EM, Chisti Y. Production of lovastatin by *Aspergillus terreus*: effects of the C: N ratio and the principal nutrients on growth and metabolite production. Enzyme Microb. Techol. 2003;33: 270-277.
12. Mitchell NJ, Bowers E, Hurburgh C, Wu F. Potential economic losses to the US corn industry from aflatoxin contamination. Food Addit. Contam. Part A. 2016;33: 540-550.
13. Hill RA, Blankenship PD, Cole RJ, Sanders TH. Effects of soil moisture and temperature on preharvest invasion of peanuts by the *Aspergillus flavus* group and subsequent aflatoxin development. Appl. Environ. Microbiol. 1983;45: 628-633.
14. Scully BT, Krakowsky MD, Ni X, Wilson JP, Lee RD, Guo B. Preharvest aflatoxin contamination of corn and other grain crops grown on the US Southeastern Coastal Plain. Toxin Rev. 2009;28: 169-179.
15. Fountain JC, Scully BT, Chen ZY, Gold SE, Glenn AE, Abbas HK, Lee RD, Kemerait RC, Guo B. Effects of hydrogen peroxide on different toxigenic and atoxigenic isolates of *Aspergillus flavus*. Toxins. 2015;7: 2985-2999.
16. Yan S, Liang Y, Zhang J, Liu CM. *Aspergillus flavus* grown in peptone as the carbon source exhibits spore density-and peptone concentration-dependent aflatoxin biosynthesis. BMC Microbiol. 2012;12: 106. DOI: doi.org/10.1186/1471-2180-12-106
17. Xue HQ, Isleib TG, Payne GA, Wilson RF, Novitzky WP, O'Brian G. Comparison of aflatoxin production in normal-and high-oleic backcross-derived peanut lines. Plant Dis. 2003;87: 1360-1365.
18. Zeringue HJ, Brown RL, Neucere JN, Cleveland TE. Relationships between C6− C12 alkanal and alkenal volatile contents and resistance of maize genotypes to *Aspergillus flavus* and aflatoxin production. J. Ag. Food Chem. 1996;44: 403-407.
19. Burow GB, Nesbitt TC, Dunlap J, Keller NP. Seed lipoxygenase products modulate *Aspergillus* mycotoxin biosynthesis. Mol. Plant Microbe Interact. 1997;10: 380-387.
20. Gao X, Brodhagen M, Isakeit T, Brown SH, Göbel C, Betran J, Feussner I, Keller NP, Kolomiets MV. Inactivation of the lipoxygenase ZmLOX3 increases susceptibility of maize to *Aspergillus spp*. Mol. Plant Microbe Interact. 2009;22: 222-231.
21. Yang L, Fountain JC, Ji P, Ni X, Chen S, Lee RD, Kemerait RC, Guo B. Deciphering drought-induced metabolic responses and regulation in developing maize kernels. Plant biotechnology journal. 2018. DOI: doi: 10.1111/pbi.12899.
22. Tsitsigiannis DI, Keller NP. Oxylipins as developmental and host–fungal communication signals. Trends Microbiol. 2007;15: 109-118.
23. Grintzalis K, Vernardis SI, Klapa MI, Georgiou CD. The role of oxidative stress in sclerotial differentiation and aflatoxin B1 biosynthesis in *Aspergillus flavus*. Appl. Environ. Microbiol. 2014; 80: 5561-5571.
24. Jayashree T, Subramanyam C. Oxidative stress as a prerequisite for aflatoxin production by *Aspergillus parasiticus*. Free Radic. Biol. Med. 2000;29: 981-985.
25. Narasaiah KV, Sashidhar RB, Subramanyam C. Biochemical analysis of oxidative stress in the production of aflatoxin and its precursor intermediates. Mycopathologia. 2006;162: 179-189.
26. Yin WB, Reinke AW, Szilagyi M, Emri T, Chiang YM, Keating AE, Pocsi I, Wang CC, Keller NP. bZIP transcription factors affecting secondary metabolism, sexual development and stress responses in *Aspergillus nidulans*. Microbiol. 2013;159: 77-88.

27. Roze LV, Laivenieks M, Hong SY, Wee J, Wong SS, Vanos B, Awad D, Ehrlich KC, Linz JE. Aflatoxin biosynthesis is a novel source of reactive oxygen species—a potential redox signal to initiate resistance to oxidative stress? Toxins. 2015;7: 1411-1430.
28. Roze LV, Chanda A, Wee J, Awad D, Linz JE. Stress-related transcription factor atfB integrates secondary metabolism with the oxidative stress response in *Aspergilli*. J. Biol. Chem. 2011;286: 35137-35148.
29. Soboń A, Szewczyk R, Różalska S, Długoński J. Metabolomics of the recovery of the filamentous fungus *Cunninghamella echinulata* exposed to tributyltin. Int. Biodeterior. Biodegradation. 2018;127: 130-138.
30. Xu Q, Fu Y, Li S, Jiang L, Rongfeng G, Huang H. Integrated transcriptomic and metabolomic analysis of *Rhizopus oryzae* with different morphologies. Process Biochem. 2018;64: 74-82.
31. Zheng H, Kim J, Liew M, Yan JK, Herrera O, Bok JW, Kelleher NL, Keller NP, Wang Y. Redox metabolites signal polymicrobial biofilm development via the NapA oxidative stress cascade in *Aspergillus*. Curr. Biol. 2015;25: 29-37.
32. Fountain JC, Bajaj P, Nayak SN, Yang L, Pandey MK, Kumar V, Jayale AS, Chitikineni A, Lee RD, Kemerait RC, Varshney RK. Responses of *Aspergillus flavus* to oxidative stress are related to fungal development regulator, antioxidant enzyme, and secondary metabolite biosynthetic gene expression. Front. Microbiol. 2016a;7: 2048. DOI: 10.3389/fmicb.2016.02048
33. Fountain JC, Bajaj P, Pandey M, Nayak SN, Yang L, Kumar V, Jayale AS, Chitikineni A, Zhuang W, Scully BT, Lee RD. Oxidative stress and carbon metabolism influence *Aspergillus flavus* transcriptome composition and secondary metabolite production. Sci. Rep. 2016b;6: 38747. DOI: 10.1038/srep38747
34. Fountain JC, Koh J, Yang L, Pandey MK, Nayak SN, Bajaj P, Zhuang WJ, Chen ZY, Kemerait RC, Lee RD, Chen S. Proteome analysis of *Aspergillus flavus* isolate-specific responses to oxidative stress in relationship to aflatoxin production capability. Sci. Rep. 2018;8: 3430. DOI: 10.1038/s41598-018-21653-x
35. Mehl HL, Cotty PJ. Variation in competitive ability among isolates of *Aspergillus flavus* from different vegetative compatibility groups during maize infection. Phytopathology. 2010;100: 150-159.
36. Mehl HL, Cotty PJ. Influence of plant host species on intraspecific competition during infection by *Aspergillus flavus*. Plant Pathol. 2013;62: 1310-1318.
37. Cotty PJ. Virulence and cultural characteristics of two *Aspergillus flavus* strains pathogenic on cotton. Phytopathology. 1989;79: 808-814.
38. Ehrlich KC, Montalbano BG, Cotty PJ. Analysis of single nucleotide polymorphisms in three genes shows evidence for genetic isolation of certain *Aspergillus flavus* vegetative compatibility groups. FEMS Microbiol. Lett. 2007;268: 231-236.
39. Chang PK, Abbas HK, Weaver MA, Ehrlich KC, Scharfenstein LL, Cotty PJ. Identification of genetic defects in the atoxigenic biocontrol strain *Aspergillus flavus* K49 reveals the presence of a competitive recombinant group in field populations. Int. J. Food Microbiol. 2012;154: 192-196.
40. Kanehisa M, Goto S. KEGG: Kyoto encyclopedia of genes and genomes. Nucleic Acids Res. 2000;28: 27-30.

41. Roze LV, Laivenieks M, Hong SY, Wee J, Wong SS, Vanos B, Awad D, Ehrlich KC, Linz JE. Aflatoxin biosynthesis is a novel source of reactive oxygen species—a potential redox signal to initiate resistance to oxidative stress? Toxins. 2015;7: 1411-1430.
42. Meletiadis J, Meis JF, Mouton JW, Verweij PE. Analysis of growth characteristics of filamentous fungi in different nutrient media. J. Clin. Microbiol. 2001;39: 478-484.
43. Clevström G, Ljunggren H, Tegelström S, Tideman K. Production of aflatoxin by an *Aspergillus flavus* isolate cultured under a limited oxygen supply. Appl. Environ. Microbiol. 1983;46: 400-405.
44. Sawa K, Uematsu T, Korenaga Y, Hirasawa R, Kikuchi M, Murata K, Zhang J, Gai X, Sakamoto K, Koyama T, Satoh T. Krebs cycle intermediates protective against oxidative stress by modulating the level of reactive oxygen species in neuronal ht22 cells. Antioxidants. 2017;6: 21. DOI: 10.3390/antiox6010021.
45. Dijkema C, Kester, HCM, Visser J. 13C NMR studies of carbon metabolism in the hyphal fungus *Aspergillus nidulans*. Proc. Natl. Acad. Sci. USA. 1985:82: 14-18.
46. Lima PS, Casaletti L, Bailao AM, Vasconcelos ATR, Fernandes GR, Soares CMA. Transcriptional and proteomic responses to carbon starvation in Paracoccidioides. PLoS Negl. Trop. Dis. 2014:8: e2855. DOI: 10.1371/journal.pntd.0002855
47. Kapoor D, Sharma R, Handa N, Kaur H, Rattan A, Yadav P, Gautam V, Kaur R, Bhardwaj R. Redox homeostasis in plants under abiotic stress: role of electron carriers, energy metabolism mediators and proteinaceous thiols. Front. Environ. Sci. 2015;3: 13. DOI: 10.3389/fenvs.2015.00013
48. Campbell K, Vowinckel J, Keller MA, Ralser M. Methionine metabolism alters oxidative stress resistance via the pentose phosphate pathway. Antioxid. Redox Signal. 2016;24: 543-547.
49. Juhnke H, Krems B, Kötter P, Entian KD. Mutants that show increased sensitivity to hydrogen peroxide reveal an important role for the pentose phosphate pathway in protection of yeast against oxidative stress. Mol. Gen. Genet. 1996;252: 456-464.
50. Huang JQ, Jiang HF, Zhou YQ, Lei Y, Wang SY, Liao BS. Ethylene inhibited aflatoxin biosynthesis is due to oxidative stress alleviation and related to glutathione redox state changes in *Aspergillus flavus*. Int. J. Food Microbiol. 2009;130:17-21.
51. Kletzien RF, Harris PK, Foellmi LA. Glucose-6-phosphate dehydrogenase: a "housekeeping" enzyme subject to tissue-specific regulation by hormones, nutrients, and oxidant stress. FASEB J. 1994;8: 174-181.
52. Shih CN, Marth EH. Aflatoxin formation, lipid synthesis, and glucose metabolism by *Aspergillus parasiticus* during incubation with and without agitation. Biochim. Biophys. Acta Gen. Subj. 1974;338: 286-296.
53. Chen C, Dickman MB. Proline suppresses apoptosis in the fungal pathogen *Colletotrichum trifolii*. Proc. Natl. Acad. Sci. USA. 2005;102: 3459-3464.
54. Szabados L, Savoure A. Proline: a multifunctional amino acid. Trends Plant Sci. 2010;15: 89-97.
55. Zhang K, Yuan X, Zang J, Wang M, Zhao F, Li P, Cao J, Han J, Xing J, Dong J. The kynurenine 3-monooxygenase encoding gene, BcKMO, is involved in the growth, development, and pathogenicity of *Botrytis cinerea*. Front. Microbiol. 2018;9: 1039. DOI: 10.3389/fmicb.2018.01039.

56. Breitenbach M, Weber M, Rinnerthaler M, Karl T, Breitenbach-Koller L. Oxidative stress in fungi: its function in signal transduction, interaction with plant hosts, and lignocellulose degradation. Biomolecules. 2015;5: 318-342.
57. Thön M, Al-Abdallah Q, Hortschansky P, Brakhage AA. The thioredoxin system of the filamentous fungus *Aspergillus nidulans* impact on development and oxidative stress response. J. Biol. Chem. 2007;282: 27259-27269.
58. Horn BW. Biodiversity of *Aspergillus* section Flavi in the United States: a review. Food Addit. Contam. 2007;24: 1088-1101.
59. Jong CJ, Azuma J, Schaffer S. Mechanism underlying the antioxidant activity of taurine: prevention of mitochondrial oxidant production. Amino Acids. 2012;42: 2223-2232.
60. Valdés-Santiago L, Ruiz-Herrera J. Stress and polyamine metabolism in fungi. Front. Chem. 2014;1: 42. DOI: 10.3389/fchem.2013.00042.
61. Avila MA, Garcıa-Trevijano ER, Lu SC, Corrales FJ, Mato JM. Methylthioadenosine. Int. J. Biochem. Cell Biol. 2004;36: 2125-2130.
62. Fanelli C, Fabbri AA. Relationship between lipids and aflatoxin biosynthesis. Mycopathologia. 1989;107: 115-120.
63. Calvo AM, Hinze LL, Gardner HW, Keller NP. Sporogenic effect of polyunsaturated fatty acids on development of *Aspergillus spp*. Appl. Environ. Microbiol. 1999;65: 3668-3673.
64. Affeldt KJ, Brodhagen M, Keller NP. *Aspergillus* oxylipin signaling and quorum sensing pathways depend on G protein-coupled receptors. Toxins. 2012;4: 695-717.
65. Fischer GJ, Keller NP. Production of cross-kingdom oxylipins by pathogenic fungi: An update on their role in development and pathogenicity. J. Microbiol. 2016;54: 254-264.
66. Rodríguez-Vargas S, Sánchez-García A, Martínez-Rivas JM, Prieto JA, Randez-Gil F. Fluidization of membrane lipids enhances the tolerance of *Saccharomyces cerevisiae* to freezing and salt stress. Appl. Environ. Microbiol. 2007;73: 110-116.
67. Yasmin S, Alcazar-Fuoli L, Gründlinger M, Puempel T, Cairns T, Blatzer M, Lopez JF, Grimalt JO, Bignell E, Haas H. Mevalonate governs interdependency of ergosterol and siderophore biosyntheses in the fungal pathogen *Aspergillus fumigatus*. Proc. Natl Acad. Sci. USA. 2012;109: 497-504.
68. Singh D, Lee S, Lee CH. Fathoming *Aspergillus oryzae* metabolomes in formulated growth matrices. Crit. Rev. Biotechnol. 2018. DOI: 10.1080/07388551.2018.1490246.
69. Fountain J, Scully B, Ni X, Kemerait R, Lee D, Chen ZY, Guo B. Environmental influences on maize-*Aspergillus flavus* interactions and aflatoxin production. Front. Microbiol. 2014;5: 40. DOI: 10.3389/fmicb.2014.00040.
70. Fernandez O, Urrutia M, Bernillon S, Giauffret C, Tardieu F, Le Gouis J, Langlade N, Charcosset A, Moing A, Gibon Y. Fortune telling: metabolic markers of plant performance. Metabolomics. 2016;12: 158. DOI: 10.1007/s11306-016-1099-1.
71. Lin Z, Zhang X, Wang Z, Jiang Y, Liu Z, Alexander D, Li G, Wang S, Ding Y. Metabolomic analysis of pathways related to rice grain chalkiness by a notched-belly mutant with high occurrence of white-belly grains. BMC Plant Biol. 2017;17: 39. DOI: 10.1186/s12870-017-0985-7
72. Lawton KA, Berger A, Mitchell M, Milgram KE, Evans AM, Guo L, Hanson RW, Kalhan SC, Ryals JA, Milburn MV. Analysis of the adult human plasma metabolome. Pharmacogenomics. 2008;9: 383-397.

73. Rao J, Cheng F, Hu C, Quan S, Lin H, Wang J, Chen G, Zhao X, Alexander D, Guo L, Wang G. Metabolic map of mature maize kernels. Metabolomics. 2014;10: 775-787.
74. Conesa A, Götz S, García-Gómez JM, Terol J, Talón M, Robles M. Blast2GO: a universal tool for annotation, visualization and analysis in functional genomics research. Bioinformatics. 2005;21: 3674-3676.

802 **Figure Legends**

803 **Figure 1.** Growth curve analysis of *Aspergillus flavus* isolates AF13 and NRRL3357 under
804 increasing oxidative stress and conidial concentration. The growth of AF13 (A, C) and
805 NRRL3357 (B, D) were examined under increasing H_2O_2 concentrations in YES medium
806 inoculated with either 2.0 x 10^4 (A, B) or 8.0 x 10^4 conidia/mL (C, D) by monitoring absorbance
807 at 405 nm over 100 hours. A threshold of 0.2 was selected for growth initiation timing which
808 corresponded with linear phase initiation for both isolates in most conditions and is indicated by
809 the dashed red line. Error bars represent standard deviation. No growth was detected at H_2O_2
810 concentrations >15mM in NRRL3357 with earlier growth initiation detected at higher conidia
811 concentrations.

812

813 **Figure 2.** Principal components analysis (PCA) of metabolite accumulation. A4N, A4Y, A7N,
814 and A7Y refer to AF13 at 4 and 7 DAI with and without 15mM H_2O_2 treatment. N4N, N4Y,
815 N7N, and N7Y refer to the same for NRRL3357. Dark blue points correspond with AF13 with
816 no stress and light blue points refer to AF13 with stress. Orange points correspond with
817 NRRL3357 with no stress and light orange points refer to NRRL3357 with stress. Circles
818 represent samples at 4 DAI and triangles represent samples at 7 DAI.

819

820 **Figure 3.** Differential accumulation of compounds involved in carbohydrate metabolism,
821 glutathione metabolism, and amino acid biosynthesis. Heatmaps located at each metabolite
822 represent the changes in metabolite accumulation in response to oxidative stress in AF13 and
823 NRRL3357 at 4 and 7 DAI. Red and green indicate significant increases and decreases in
824 metabolite levels, respectively ($p < 0.05$). Light red and light green indicate marginally

825 significant increases and decreases in metabolite levels, respectively ($0.05 < p < 0.10$). Grey
826 represents no significant changes.
827
828 **Figure 4.** Differential accumulation of compounds involved in polyamine and sulfur
829 metabolism. Heatmaps located at each metabolite represent the changes in metabolite
830 accumulation in response to oxidative stress in AF13 and NRRL3357 at 4 and 7 DAI. Red and
831 green indicate significant increases and decreases in metabolite levels, respectively ($p < 0.05$).
832 Light red and light green indicate marginally significant increases and decreases in metabolite
833 levels, respectively ($0.05 < p < 0.10$). Grey represents no significant changes.
834
835 **Figure 5.** Differential accumulation of compounds involved in lipid metabolism. Heatmaps
836 located at each metabolite represent the changes in metabolite accumulation in response to
837 oxidative stress in AF13 and NRRL3357 at 4 and 7 DAI. Red and green indicate significant
838 increases and decreases in metabolite levels, respectively ($p < 0.05$). Light red and light green
839 indicate marginally significant increases and decreases in metabolite levels, respectively ($0.05 <$
840 $p < 0.10$). Grey represents no significant changes.
841
842

Supplemental Figure Legends

Figure S1. Metabolomics experiment design. Two isolates of *Aspergillus flavus*, AF13 (highly aflatoxigenic and oxidative stress tolerant) and NRRL3357 (moderate to highly aflatoxigenic and moderately oxidative stress tolerant), were grown in yeast extract sucrose (YES) medium supplemented with either 0 or 15 mM H_2O_2. Samples were collected at 4 and 7 days after inoculation (DAI). Five biological replicates (n = 5, N = 40) were performed for each isolate, treatment, and time point combination. Statistical comparisons are indicated by the colored arrows with blue indicating oxidative stress effect comparisons, red indicating time effects, and green indicating isolate/genotype effects.

861 **Tables**

Table 1. Numbers of significantly, differentially accumulating metabolites.

Effects	Comparison	Total Sig. Met.	Sig. Increased	Sig. Decreased
Time	A7N / A4N	257	58	199
	A7Y / A4Y	268	108	160
	N7N / N4N	243	51	192
	N7Y / N4Y	261	118	143
Stress	A4Y / A4N	111	27	84
	A7Y / A7N	47	34	13
	N4Y / N4N	223	90	133
	N7Y / N7N	90	65	25
Isolate	A4N / N4N	143	95	48
	A7N / N7N	97	50	47
	A4Y / N4Y	220	128	92
	A7Y / N7Y	96	42	54

Comparison nomenclature: AF13 (A), NRRL3357 (N), DAI (4 and 7), without H_2O_2 (N), and with H_2O_2 (Y).

862

863

864

865

866

867

868

869

870

871

872

873

874

875

Figures

Figure 1

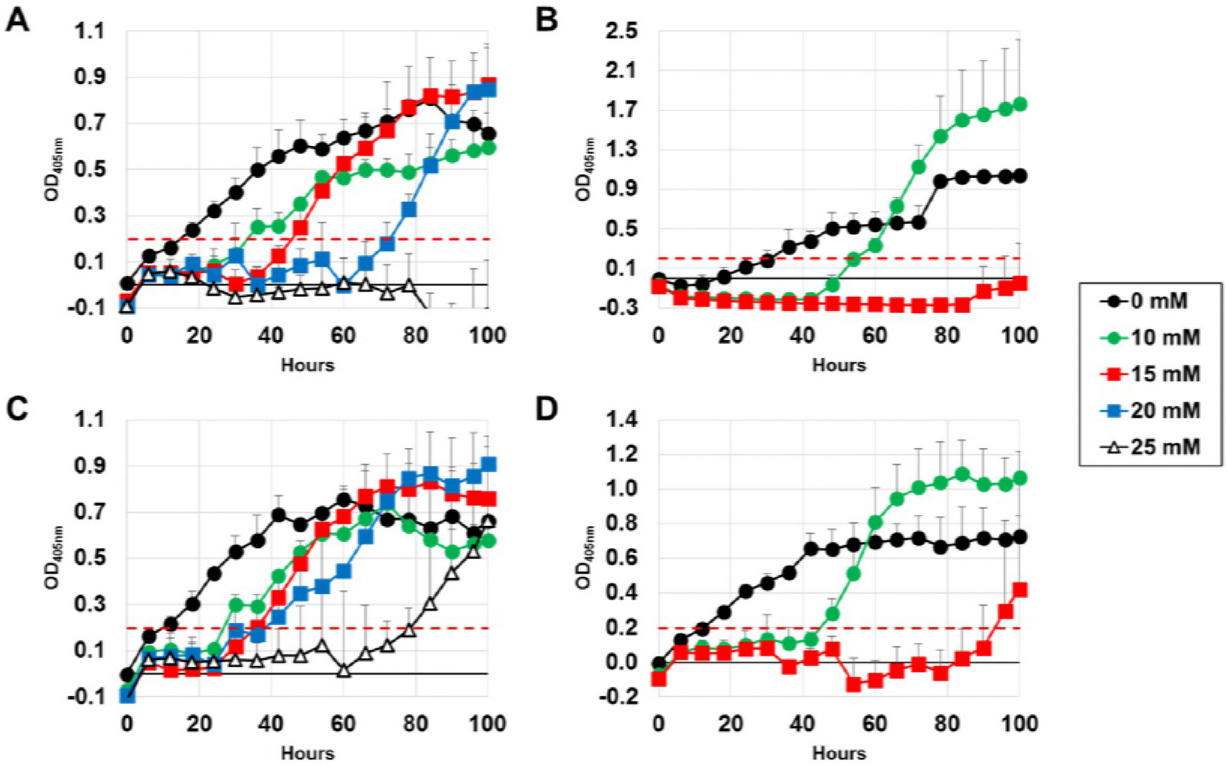

889 **Figure 2**

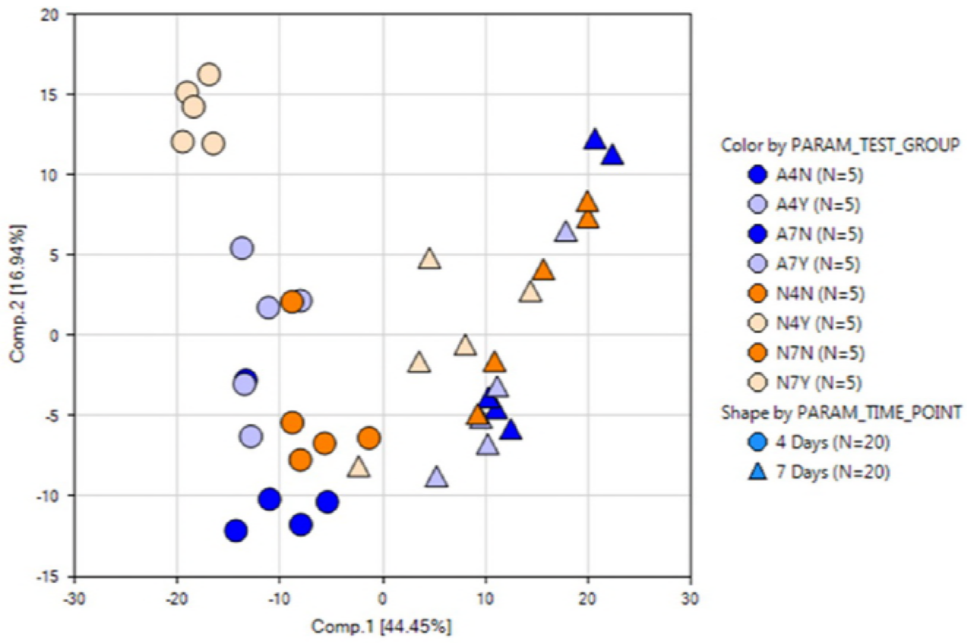

890

891

892

893

894

895

896

897

898

899

900

901

902

903

904 **Figure 3**

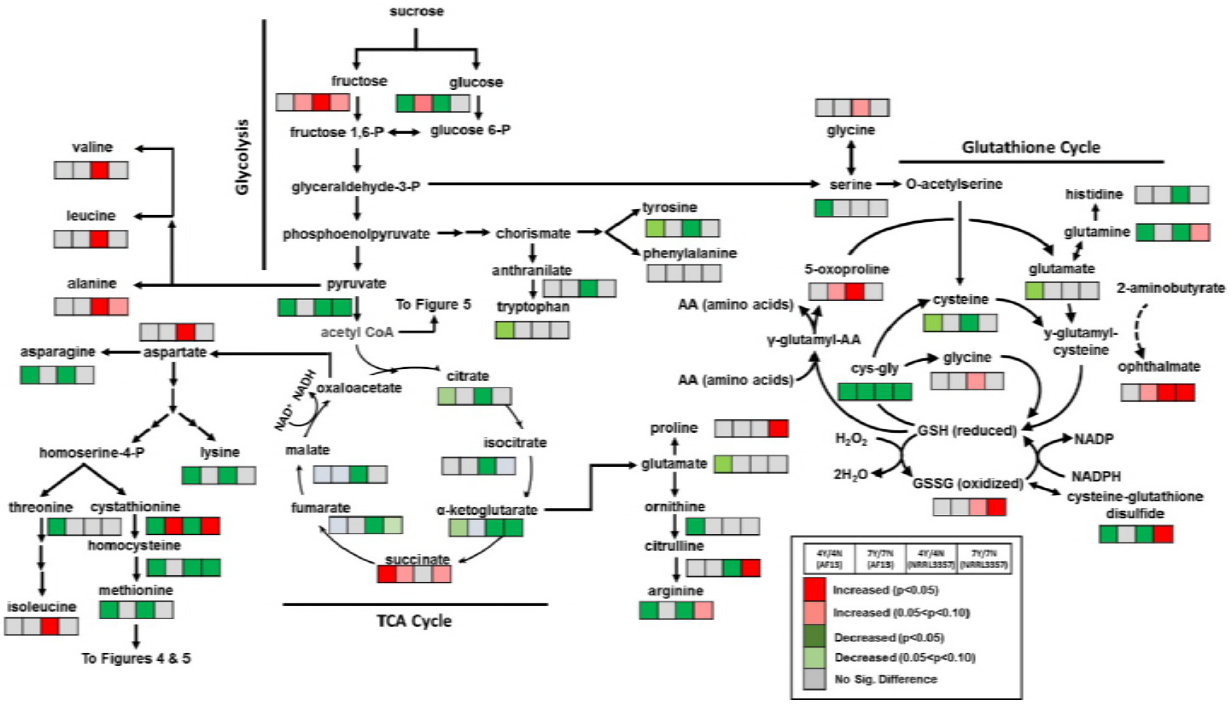

905

906

907

908

909

910

911

912

913

914

915

916

917

Figure 4

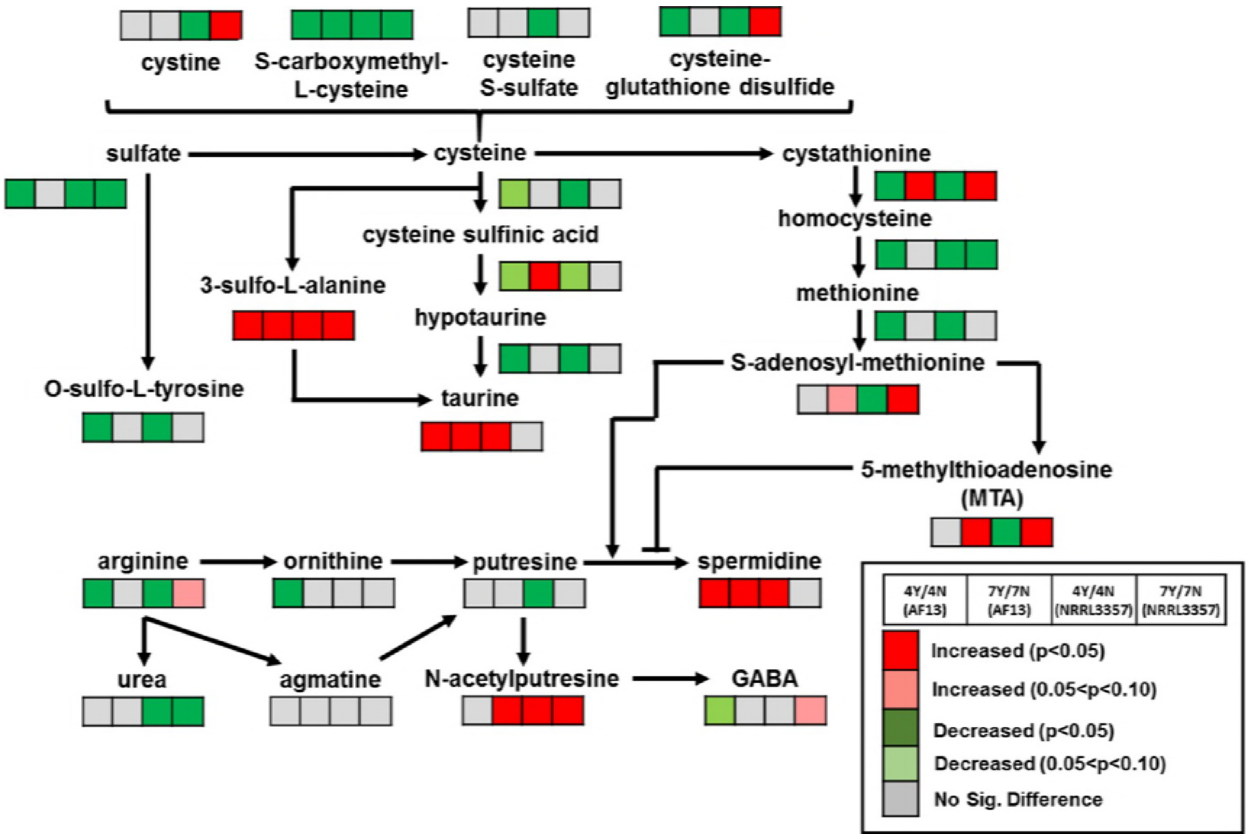

931 **Figure 5**

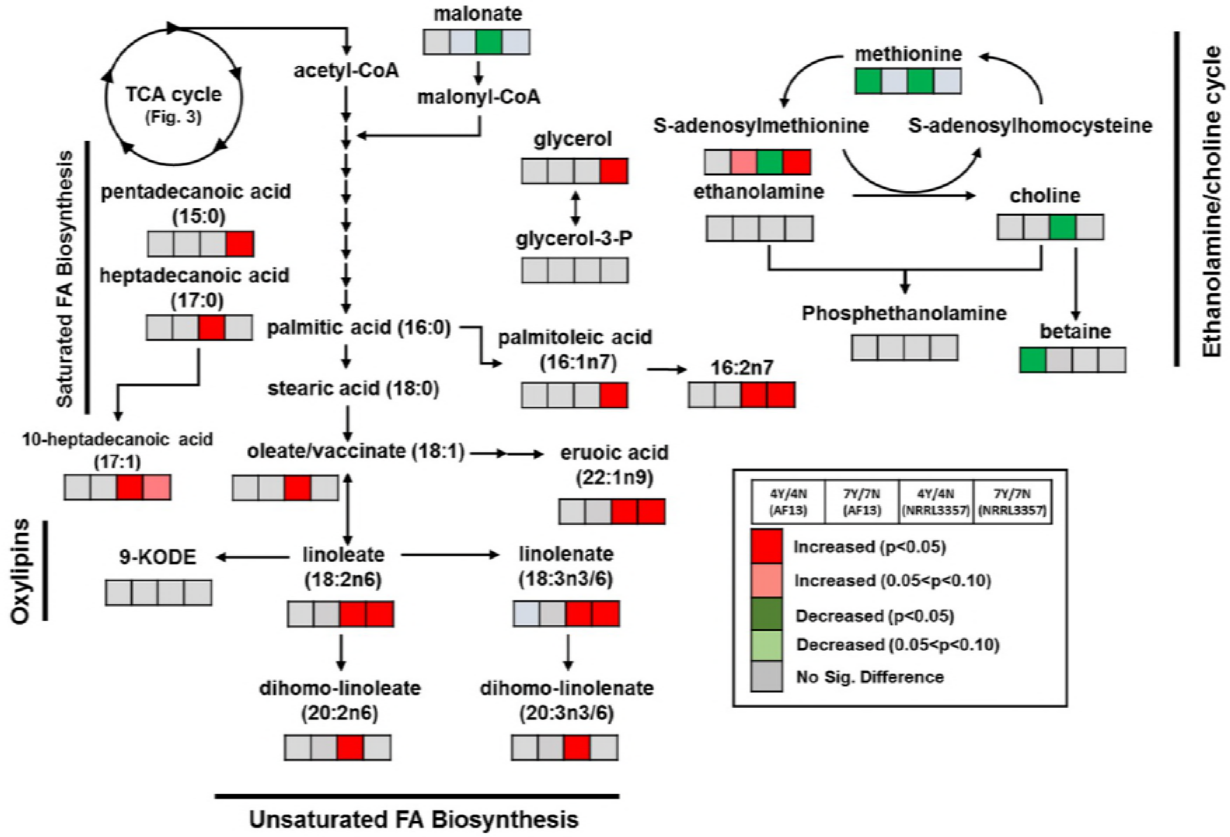

932

933

934

935

936